PHYSICAL REVIEW B **85**, 020301(R) (2012)

Broadband cloaking of bending waves via homogenization of multiply perforated radially symmetric and isotropic thin elastic plates

Mohamed Farhat,[1] Sebastien Guenneau,[2] and Stefan Enoch[2]

[1]*Institute of Condensed Matter Theory and Solid State Optics, Abbe Center of Photonics, 7 Friedrich-Schiller-Universität Jena, D-07743 Jena, Germany*

[2]*Institut Fresnel, CNRS, Aix-Marseille Université, Campus universitaire de Saint-Jérôme, F-13013 Marseille, France*

(Received 23 December 2011; revised manuscript received 18 January 2012; published 30 January 2012)

A cylindrical cloak is designed to control the bending waves propagating in isotropic thin plates. This is achieved through homogenization of a multiply perforated coating of isotropic homogeneous elastic material, which greatly simplifies the design of the multilayered cloak we proposed [Phys. Rev. Lett. **103**, 024301 (2009)]. We first derive the homogenized biharmonic equation, which involves an anisotropic Young's modulus and an isotropic mass density. We then numerically show that a clamped obstacle is cloaked over a finite range of frequencies for an acoustic source located a couple of wavelengths away from its surrounding cloak. The reduced backward and forward scattering is confirmed by both the profile of the total field computed along a line passing through the source and the center of the cloak (near field confirmation), and the computation of the scattered far field.

DOI: 10.1103/PhysRevB.85.020301 PACS number(s): 62.30.+d, 46.40.−f, 43.40.+s

Introduction. Transformation-based solutions to the conductivity and Maxwell's equations in curvilinear coordinate systems, recently reported by Greenleaf *et al.*,[1] Pendry *et al.*,[2] and Leonhardt,[3] have paved the way toward a better control of acoustic and electromagnetic waves around arbitrarily sized and shaped solids. The experimental validation of these theoretical considerations was given by Schurig *et al.*,[4] who used a cylindrical cloak consisting of concentric arrays of split ring resonators. This cloak makes a copper cylinder invisible to an incident plane wave at 8.5 GHz, as predicted by the numerical simulations. This experiment has since then fueled the interest in the field of transformation optics.

However, Milton *et al.*[5] have shown that the elasticity equations are not invariant under coordinate transformations and consequently, that if cloaking exists for such classes of waves, it would be of a different nature than its acoustic and electromagnetic counterparts.

A systematic investigation of acoustic cloaking started with Cummer and Schurig,[6] who analyzed the two-dimensional cloaking for pressure waves in a transversely anisotropic fluid by exploiting the analogy with TE electromagnetic waves. Chen and Chan[7] and Cummer *et al.*[8] further noticed that a three-dimensional (3D) acoustic cloaking for pressure waves in a fluid can be envisaged since the wave equation retains its form under geometric changes.

But when one moves to the area of coupled pressure and shear elastic waves, the isomorphism between the (tensor) governing equations and the wave equation is lost and computations become more involved. Norris investigated some general types of acoustic cloaks with finite mass consisting of so-called pentamode materials, which display an anisotropic stiffness.[9] Brun *et al.* studied a cylindrical cloak for in-plane elastic waves, which is described by a rank-4 (nonsymmetric) elasticity tensor with 2^4 entries and an isotropic density.[10] Whereas the former structured metamaterial might already represent a technological challenge for mechanical engineers, the latter proposal imposes even more severe constraints on the material parameters. Moreover, the required material properties for a three-dimensional elastic cloak remain elusive thus far, as these would involve a rank-4 elasticity tensor with up to 3^4 spatially varying nonvanishing entries. However, in the special case of thin-elastic plates, it has been shown[11] that the elasticity tensor can be represented in a cylindrical basis by a diagonal matrix with two (spatially varying) nonvanishing entries. One can easily mimic such tensors by structuring the plate with concentric layers of isotropic homogeneous material, e.g., polymers, and this leads to ultrabroadband cloaking.[12] It seems therefore quite natural to start designing such a cloak for flexural waves before investigating the control of in-plane elastic waves also involved in seismic events. This route has been experimentally validated this year for frequencies in the range 200–400 Hz by Stenger, Wilhelm, and Wegener[13] for a cloak consisting of 20 concentric rings of 16 different metamaterials, each being a tailored composite of polyvinylchlorid and polydimethylsiloxan, following our theoretical proposal.[12]

We note that such an avenue toward broadband cloaking was opened by Torrent and Sanchez-Dehesa[14] and Cheng *et al.*[15] in the context of acoustic waves for concentric multilayered cloaks behaving as anisotropic fluids in the homogenization limit. Using a similar approach, Farhat *et al.*[16] demonstrated cloaking of surface liquid waves for a microstructured metallic cloak via effective anisotropic shear viscosity, while Chen *et al.*[17] achieved rotating effects via effective anisotropic depth, both models being experimentally validated at Hertz frequencies. It is the latter work which we would like to extend to flexural waves in this Rapid Communication, thanks to the similarities between surface liquid waves and surface elastic waves.

Description of the proposed method of elastic cloaking. In this Rapid Communication, we show that a heterogeneous orthotropic cloak can be designed via a radially symmetric multilayered cloak with a constant isotropic Young's modulus E and mass density ρ to make an object surrounded by such a coat neutral for flexural waves in thin elastic plates. This is

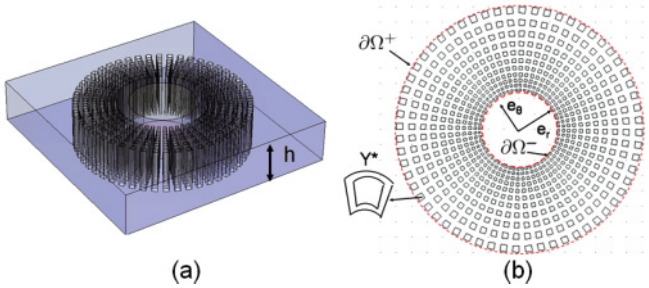

FIG. 1. (Color online) Geometry of the structured cloak. (a) 3D view: The thickness h of the plate of density ρ_0 and flexural rigidity D_0 is assumed to be small compared to the incident wavelength $\lambda = 2\pi/\omega = 2\pi\sqrt{\rho_0 h}/(\beta_0^2\sqrt{D_0})$ of the flexural wave, where β_0 is the reduced wave frequency. The typical cross-sectional size of perforations is also small compared to λ. The large cylinder in the center of the structure represents the invisibility region and could consist either of air (in which case one sets clamped or stress-free boundary conditions on its boundary) or the same material as the plate (in which case one sets transmission boundary conditions on its boundary). (b) View from above: The inner and outer (virtual) boundaries $\partial\Omega^-$ and $\partial\Omega^+$ of the cloak Ω are represented by red dotted curves. The cloak is evenly divided (in a polar coordinate axis) in curved sectors Y^*, which are basic cells Y with an air hole S (a perforation of the thin plate).

achieved thanks to periodic perforations (air holes) in the plate (see Fig. 1).

Homogenization of a multiply perforated thin plate. The equations for bending of plates are well known and can be found in many textbooks, such as those of Timoshenko or Graff.[18,19] The wavelength λ is supposed to be large enough compared to the thickness of the plate h and small compared to its in-plane dimension L, i.e., $h \ll \lambda \ll L$. In this case we can adopt the hypothesis of the theory of von Karman.[18,19]

When the bending wave penetrates the structured cloak Ω, whose geometry is shown in Fig. 1(b), it undergoes fast periodic oscillations. To filter these oscillations, we consider an asymptotic expansion of the associated vertical displacement U_η solution of (1) in terms of a macroscopic (or slow) variable $\mathbf{x} = (r,\theta)$ (in polar coordinates—see Fig. 1) and a microscopic (or fast) variable $\mathbf{x}_\eta = (\frac{r}{\eta},\theta)$, where η is a small positive real parameter.

With all the above assumptions, the out-of-plane displacement $\mathbf{u}_\eta = [0,0,U_\eta(r,\theta)]$ in the x_3 direction (along the vertical axis) is the solution of

$$\rho_\eta^{-1}\nabla\cdot\left[\zeta_\eta^{-1}\nabla\left(\rho_\eta^{-1}\nabla\cdot\left[\zeta_\eta^{-1}\nabla U_\eta\right]\right)\right] - \beta_0^4 U_\eta = 0, \quad (1)$$

inside the heterogeneous isotropic cloak Ω, where

$$\zeta_\eta = E^{-1/2}\left(\frac{r}{\eta}\right) \quad \text{and} \quad \rho_\eta = \rho^{1/2}\left(\frac{r}{\eta}\right).$$

Here $\zeta_\eta^{-1} = 0$ and $\rho_\eta = 0$ inside freely vibrating inclusions (plate perforations) and 1 elsewhere. Furthermore, $\beta_0^4 = \omega^2\,\rho_0 h/D_0$, where D_0 is the flexural rigidity of the plate, ρ_0 its density, and h its thickness.

Using multiscale techniques described in Ref. 20, we find that the homogenized system takes the form

$$\nabla\cdot([\xi_{\rm hom}]^{-1}\nabla(\nabla\cdot[[\xi_{\rm hom}]^{-1}\nabla U_{\rm hom}])) - \beta_{\rm hom}^4\, U_{\rm hom} = 0, \quad (2)$$

which is the homogenized biharmonic equation with $\beta_{\rm hom} = {\rm area}(Y^*)^{1/2}\beta_0$ and the rank-2 tensor $[\xi_{\rm hom}]$ (an anisotropic Young's modulus) given by

$$[\xi_{\rm hom}] = \frac{1}{{\rm area}(Y^*)}\begin{pmatrix} {\rm area}(Y^*) - \psi_{rr} & \psi_{r\theta} \\ \psi_{\theta r} & {\rm area}(Y^*) - \psi_{\theta\theta}\end{pmatrix}. \quad (3)$$

Here Y^* denotes the region surrounding a freely vibrating inclusion in an elementary cell of the periodic array, and ψ_{ij} represent corrective terms defined by

$$\forall i,\ j \in \{r,\theta\},\ \psi_{ij} = -\int_{\partial S}\Psi_i n_j ds, \quad (4)$$

where $\mathbf{n}$ is the unit outward normal to the boundary ∂S of the inclusion.

Furthermore, Ψ_j, $j \in \{r,\theta\}$, are periodic potentials which are unique solutions (up to an additive constant) of the following two biharmonic equations $(\mathcal{K}_j)$:

$$(\mathcal{K}_j):\ \nabla^4\Psi_j = 0 \text{ in } Y^*, \quad (5)$$

which are supplied with the effective boundary condition $\frac{\partial\Psi_j}{\partial n} = \frac{\partial^2\Psi_j}{\partial n^2} = \frac{\partial^3\Psi_j}{\partial n^3} = -\mathbf{n}\cdot\mathbf{e}_j$ on the boundary ∂S of the inclusion. Here, $\mathbf{e}_r$ and $\mathbf{e}_\theta$ denote the vectors of the basis in polar coordinates (r,θ).

Solving (5) numerically with finite elements, computing the line integral (4), and inserting the resulting corrective terms in (3), we obtain

$$[\xi_{\rm hom}] = \frac{1}{{\rm area}(Y^*)}\begin{pmatrix} {\rm area}(Y^*) + 0.7 & 0 \\ 0 & {\rm area} + 7.2\end{pmatrix}, \quad (6)$$

which shows that the effective coating is strongly anisotropic along the azimuthal θ direction and it further varies along the radial r direction.

It is interesting to note that the expression of the anisotropic Young's modulus (6) has the same structure as for the case of the structured cloak we introduced in the context of linear water waves.[16] However, we stress that the annex problem (5) is a biharmonic equation, while it was a harmonic equation in Ref. 16. As the proverb says, the same cause produces the same effect: The artificial anisotropy is again responsible for the cloaking effect.

Two-step homogenization approach to elastic cloaking. We now note that the coordinate transformation $r' = R_1 + r\frac{R_2-R_1}{R_2}$ (Refs. 1 and 2) can compress the region $r < R_2$ into the ring $R_1 < r < R_2$, provided that the thin plate is described by the following material parameters:[11]

$$E_r = \left(\frac{r-R_1}{r}\right)^2, \quad E_\theta = \left(\frac{r}{r-R_1}\right)^2, \quad \rho = \left(\frac{R_2}{R_2-R_1}\right)^4\left(\frac{r-R_1}{r}\right)^2, \quad (7)$$

where R_1 and R_2 are the interior and the exterior radii of the elastic coat of thickness h. This ideal cloak is therefore not only anisotropic, but also spatially varying along the radius r.

To mimic these ideal parameters, we proceed in two steps, as follows:[15] We first approximate the cloak obtained by geometric transformation by a multilayered cloak with M

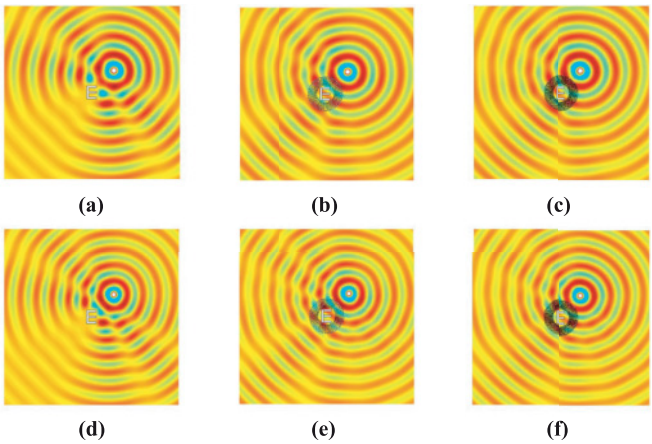

FIG. 2. (Color online) Real part of the displacement field U' distribution in the vicinity of the E-shaped clamped obstacle on its own (a), (d), when it is surrounded by a cloak with 100 perforations (b), (e) and when it is surrounded by a cloak with 200 perforations (c), (f). The source is located at point (0.5,0.5) and its wavelength is $\lambda_0 = 2\pi/\beta_0 = 2\pi/15 = 0.42$ in (a)–(c) and $\lambda_0 = 2\pi/\beta_0 = 2\pi/17.5 = 0.36$ in (d)–(f). The inner and outer radii of the cloak are $R_1 = 0.2$ and $R_2 = 0.39$ and it consists of six rows of sectors (perforations) in (b) and (d) while the inner and outer radii of the cloak are $R_1 = 0.2$ and $R_2 = 0.4$ and it consists of 11 rows of sectors (perforations) in (c) and (f). We note that the scattering is minimized in (c) and (f), i.e., for the cloak with 200 sectors.

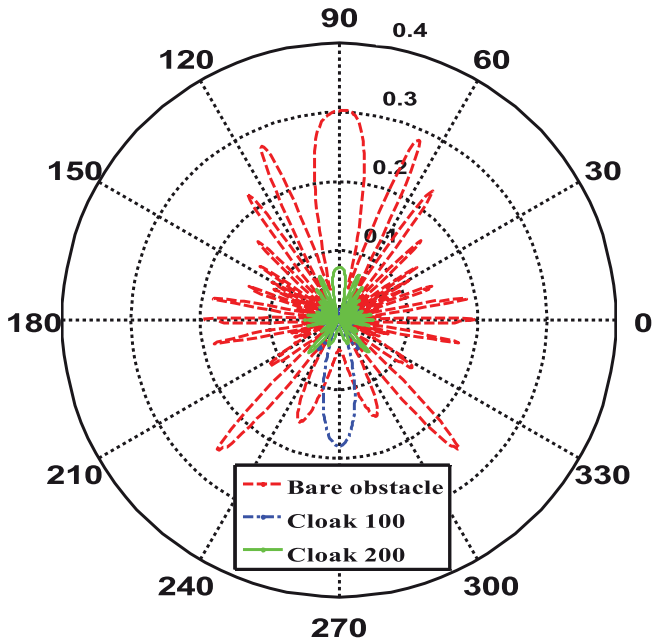

FIG. 3. (Color online) Far-field computations of the scattered flexural wave for a bare obstacle (red dashed curve), for a cloak with 100 perforations (blue dashed-dotted curve) and for a cloak with 200 perforations (green solid curve). This demonstrates that the larger is the number of small perforations, the more reduced is the scattering.

anisotropic homogeneous concentric layers. We then approximate each layer $i, i = 1, \ldots, M$ by N thin isotropic perforated layers through the homogenization process described above. This means the overall number NM of isotropic layers can be fairly large.

Numerical simulation of elastic cloaking. We now turn to the numerical analysis of the field radiated by a point source vibrating harmonically in the x_3 direction and generating a harmonic vibration on the plate. Note that all the lengths are in arbitrary units (e.g., mm). This point source is located at the point (0.5,0.5) in the vicinity of a clamped obstacle shaped as the letter E on its own and when it is surrounded by a perforated cloak within the annular region of radii $R_1 = 0.2$ and $R_2 = 0.39$ when it is made of six rows with 100 perforations [see Figs. 2(b) and 2(e)], and radii $R_1 = 0.2$ and $R_2 = 0.4$ when it is made of six rows with 200 perforations [see Figs. 2(c) and 2(f)]. Every cloak is centered about the origin. Its elastic parameters are characterized by a spatially varying scalar density ρ and a spatially varying rank-2 tensor $[E]$ given by (7). Physically speaking, the panels in Fig. 2 represent the real part of the vertical displacement U' in the presence of the point source that is nothing but the bending waves at the instant $t = 0$. As predicted by homogenization theory, the vertical displacement outside the cloak is nearly identical to the one we obtain when the plate is homogeneous (without any obstacle and cloak), except for a phase shift associated with the longer trajectory of the flexural wave (which is detoured around the cloak instead of traveling right through it). Moreover, when we increase the number of perforations, cloaking is all the more effective. Importantly, cloaking works over a finite range of frequencies (from $\beta = 15$ to 22.5), unlike for the case of invisibility cloaks with resonant elements. We note that our earlier proposal of an antiearthquake cloak[12] is very different from the current design: The former design relies upon concentric layers of various polymers, whereas the current design only requires perforations within the thin plate and is therefore far easier to implement, even if the recent experiment of Wegener's group[13] demonstrates that the former design is within technological reach.

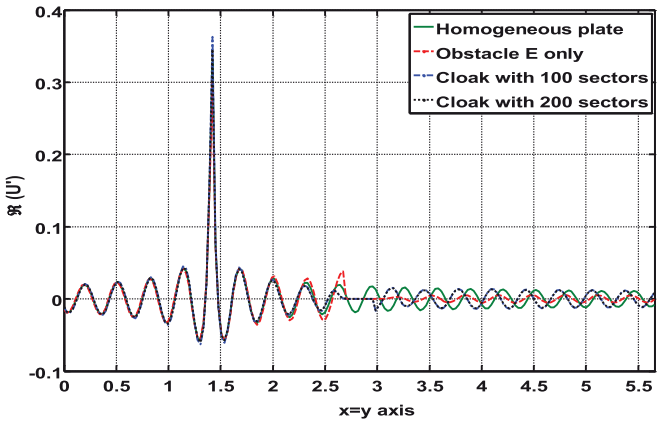

FIG. 4. (Color online) Profile of the total flexural field computed along a line passing through the source and the center of the cloak for a homogeneous plate (green solid curve), for a bare obstacle (red dashed curve), for a cloak with 100 perforations (blue dashed-dotted curve), and for a cloak with 200 perforations (black dotted curve). The amplitude of forward waves in nearly the same for the bare plate (green) and the cloaked obstacle (blue and black). However, there is a phase shift in the forward scattering between the green and blue and black curves, due to the longer path taken by flexural waves detoured around the cloaked obstacle.

Finally, Figs. 3 and 4 further confirm the much reduced scattering when the obstacle is cloaked. Importantly, the source is located in the vicinity of the cloak, whereas cloaking for the former multilayered cloak design has been demonstrated for a plane wave.

Concluding remarks. In conclusion, we have proposed a route toward elastic cloaking in thin plates. We first reviewed the relevant results published thus far on electromagnetic and acoustic cloaking. We further studied theoretically and numerically the extension of electromagnetic and acoustic cloaking mechanisms to the domain of flexural waves propagating in thin infinite elastic plates. We have proposed a design of a broadband multiperforated cloak consisting of a large number of thin homogeneous isotropic layers with periodic perforations shaped as sectors. For this, we derived the homogenized biharmonic equation using a multiscale asymptotic approach. We found that the homogenized elastic parameters are described by a rank-2 tensor (a generalized Young's modulus) and a scalar density, both of which are functions of the radius. We then performed numerical computations based on the finite-element method which proved that a rigid obstacle surrounded by a coating consisting of 100 and 200 periodic perforations is neutral (vanishing backward and forward scattering) for the bending waves generated by a point source located in its vicinity. We thus believe such a microstructured plate may have some potential applications in isolating structures from vibrations of metallic (or nonmetallic) plates in aeronautic, ship, and car industries. An experimental validation is underway in Marseille.

Acknowledgments. S.G. is thankful for an ERC funding under project ANAMORPHISM. The authors also acknowledge the help of Muamer Kadic with Fig. 1.

[1] A. Greenleaf, M. Lassas, and G. Uhlmann, Math. Res. Lett. **10**, 685 (2003).
[2] J. B. Pendry, D. Schurig, and D. R. Smith, Science **312**, 1780 (2006).
[3] U. Leonhardt, Science **312**, 1777 (2006).
[4] D. Schurig, J. J. Mock, B. J. Justice, S. A. Cummer, J. B. Pendry, A. F. Starr, and D. R. Smith, Science **314**, 977 (2006).
[5] G. W. Milton, M. Briane, and J. R. Willis, New J. Phys. **8**, 248 (2006).
[6] S. A. Cummer and D. Schurig, New J. Phys. **9**, 45 (2007).
[7] H. Chen and C. T. Chan, Appl. Phys. Lett. **91**, 183518 (2007).
[8] S. A. Cummer, B. I. Popa, D. Schurig, D. R. Smith, J. Pendry, M. Rahm, and A. Starr, Phys. Rev. Lett. **100**, 024301 (2008).
[9] A. N. Norris, Proc. R. Soc. London A **464**, 2411 (2008).
[10] M. Brun, S. Guenneau, and A. B. Movchan, Appl. Phys. Lett. **94**, 061903 (2009).
[11] M. Farhat, S. Guenneau, S. Enoch, and A. B. Movchan, Phys. Rev. B **79**, 033102 (2009).
[12] M. Farhat, S. Guenneau, and S. Enoch, Phys. Rev. Lett. **103**, 024301 (2009).
[13] N. Stenger, M. Wilhelm, and M. Wegener, Phys. Rev. Lett. **108**, 014301 (2012).
[14] D. Torrent and J. Sanchez-Dehesa, New J. Phys. **10**, 063015 (2008).
[15] Y. Cheng, F. Yang, J. Y. Xu, and X. J. Liu, Appl. Phys. Lett. **92**, 151913 (2008).
[16] M. Farhat, S. Enoch, S. Guenneau, and A. B. Movchan, Phys. Rev. Lett. **101**, 134501 (2008).
[17] H. Chen, J. Yang, J. Zi, and C. Chan, Europhys. Lett. **85**, 24004 (2009).
[18] S. Timoshenko, *Theory of Plates and Shells* (McGraw-Hill, New York, 1940).
[19] K. F. Graff, *Wave Motion in Elastic Solids* (Dover, New York, 1975).
[20] V. V. Jikhov, S. M. Kozlov, and O. A. Oleinik, *Homogenization of Differential Operators and Integral Functionals* (Springer, New York, 1994).